Wearable Technology: Developing a Skin-Like Temperature Sensor

A Technical Report submitted to the Department of Mechanical Engineering

Presented to the Faculty of the School of Engineering and Applied Science

University of Virginia • Charlottesville, Virginia

In Partial Fulfillment of the Requirements for the Degree

Bachelor of Science, School of Engineering

Spring, 2022

Technical Project Team Members

Crestienne Dechaine

Sean Donley

Emily Gresnick

Noah Klipp

Georgia White

On my honor as a University Student, I have neither given nor received unauthorized aid on this assignment as defined by the Honor Guidelines for Thesis-Related Assignments

Baoxing Xu PhD, Department of Mechanical and Aerospace Engineering

Baoxing Xu

Digitally signed by Baoxing Xu
DN: cn=Baoxing Xu, o, ou, email=bx4c@virginia.edu, c=US
Date: 2022.05.02 18:18:51 -04'00'

Abstract

Wearable sensors hold great promise for several fields, including clinical diagnostics, robotics, prosthetics and continuous health-care monitoring (Hammock et al., 2013). Our team sought to develop a skin-like temperature sensor with an original geometric design to measure temperature as a function of resistivity. The sensor was designed as a planar substrate with channels of electrically active material. Key considerations were the material selection, sensor design, and fabrication method. We utilized polydimethylsiloxane (PDMS) for the sensor's substrate and carbon nanotube (CNTs) for the electrically active material, and we investigated manufacturing methods involving 3D printing and laser cutting. Ultimately, the research culminated in a functional sensor and an improved understanding of these methods.

Contents

Introduction

The objective of this research was to develop a skin-like electronic temperature sensor and to investigate the viability of the manufacturing methods utilized in that development. Current wearable devices are typically "small, rigid blocks of wireless electronic/sensing components loosely coupled to the wrist" (Ray et al., 2019, p. 5462). Their design means the sensors are unable to form intimate skin interfaces, leading to inaccurate measurements. Skin-like wearable electronics, or e-skins, are a type of device that allows for direct application and adhesion to non-linear surfaces. Such sensors have extensive applications in robotics and the medical field. Within the medical field, these sensors have several potential uses, such as blood glucose monitoring in diabetic patients (Hammock et al., 2013, p. 6013).

The intended application of this project was to create a wearable temperature sensor that can be used on any large muscle group. Progress was made in analyzing a sensor design and two manufacturing methods. The methods included additive manufacturing using a 3D printed mold and subtractive manufacturing using a laser cutter. Fundamentally, the design permitted the analysis of two main features: the polydimethylsiloxane (PDMS) substrate and the carbon nanotube (CNT) conducting elements. The success of the design demonstrated the viability of using these features in tandem. Additionally, the primary manufacturing methods utilized in the production of the sensor worked well. Although neither method was particularly quick, they are both scalable, and increased scale would decrease the cost per unit produced.

Design Theory

Although skin-like sensors vary in their applications, they all operate on similar fundamental principles. First, they depend upon adhesion to the skin to collect data. Because of

the skin's low elastic modulus, skin-like sensors must also exhibit a low elastic modulus to maintain adhesion during physical activity (Hammock et al., 2013, p. 6000). Second, skin-like sensors operate by transducing physical stimuli into electronic signals. This operation requires miniaturized and flexible electronic sensors.

Two main techniques are employed to develop flexible devices. The simplest is simply to utilize materials that readily deform (Ray et al., 2019, pp. 5463-5467), but flexibility can also be attained by carefully fabricating deformable microstructures within the sensor (Ray et al., 2019, pp. 5467-5468). This second technique is much more complicated than the first, but it greatly increases the number of materials that can be used in skin-like sensors. In addition to flexibility, skin-like sensors must also use electronic components. Some of the more popular choices for electronic components include nanowires, graphene, and carbon nanotubes (CNTs), though alternatives are being pursued (Hammock et al., 2013, pp. 6000-6002). These general principles and methods apply to skin-like sensors in general, but the specifics of each sensor depend upon its intended use.

For our project, we chose to develop a temperature sensor. This sensor was intended to quantify changes in temperature through corresponding changes in the resistance of internal conductive elements. The change in resistance for these conducting elements depends upon the following equation:

$$\frac{R}{R_0} = \alpha T + 1 \quad (1)$$

In this equation, R is the resistance after a change in temperature, R_0 is the original resistance, α is the temperature coefficient of resistance, and T is the temperature at which R is measured (Xu, 2021).

Fabrication

The fabrication of our temperature sensor depended on several factors. The most fundamental of these was the materials used in the design, which governed the capabilities of the device and the manufacturing methods required to produce it. Once materials were selected, the physical design of the device had to be finalized within the limitations of the materials. With these in mind, specific fabrication steps could be finalized and followed to produce the sensor as efficiently as possible.

Materials-

Two primary materials were used in this design. The substrate for the sensor was chosen to be PDMS. PDMS has well-researched properties and it has commercial availability making it an affordable and popular choice. The applicable properties for PDMS included the fact that it was a transparent material with stability over a wide range of temperatures (Hammock et al., 2013, p. 6000). It was chosen to be the substrate of our sensor for these reasons. Secondly, we utilized CNTs for the active conducting material of our sensor. Not only do CNTs provide high levels of flexibility, but they are also relatively easy to integrate into designs. They also have a high surface area-to-volume ratio (Hammock et al., 2013, p. 6012), enabling them to have high sensitivity. The downsides of CNTs include a relatively high price and indefinite reports on their biocompatibility (Hammock et al., 2013, p. 6019-6020).

Structural Design-

The design for the sensor followed an iterative process. At the beginning of the year, we emphasized producing the sensor with 3D printed molds, so each member of our group designed

a preliminary mold in SolidWorks. After comparing these designs, we selected the design shown below in Figure 1 as our initial team design. With this design, the dimensions of the substrate were 89 mm x 88 mm, and the sensing channels within the substrate had square cross-sections of 1 mm x 1 mm. Additionally, the cross-sections of the connecting channels, which enabled connections from the sensing channels to the wire pads, were 1.5 mm x 1 mm, and the dimensions of the wire pads were 4 mm x 4 mm. The lip around the perimeter of the mold extended 1 mm above the bottom surface of the interior of the mold. A picture of the printed mold is shown below in Figure 1.

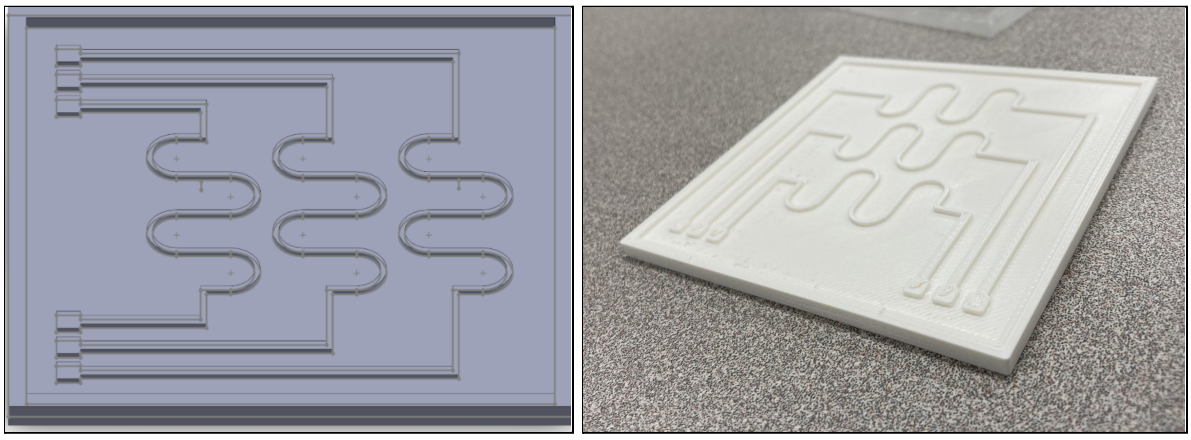

Figure 1. SolidWorks model of initial mold (left) and the 3D printed mold itself (right).

The design of the mold was relatively straightforward. It was designed to produce a uniaxial temperature sensor with a 3 x 1 array of sensing elements. The 3 x 1 array allowed for relative simplicity while also providing increased reliability and, ideally, multiple measurements. When PDMS was poured onto the mold, the raised surfaces in the interior of the mold formed channels within the PDMS, which could be filled with CNTs to form conducting segments. When the resultant sensor was stretched, the serpentine CNT channels would deform, enabling the temperature of the underlying surface to be quantified. The cross-sectional areas of the sensing elements, which were formed by the serpentine structures in the mold, were much lower

than the cross-sectional areas of the connecting pathways in order to increase the sensitivity of the device.

After initially using this design, we recognized a serious shortcoming. The lip around the perimeter of the mold was insufficiently high, and because of this, it was difficult to form a continuous layer of PDMS—PDMS would spill over the edges of the mold before the channel-forming sections of the mold were adequately covered. A potential workaround for this flaw was to pour enough PDMS to submerge the entire mold, allowing the CNT channels to form. This approach was unsuccessful, as the final thickness of the PDMS layer was inconsistent, and it also wasted a large amount of PDMS. To address this fault, we modified our mold.

In doing so, we made several changes. First, we raised the lip of the mold to 3 mm so that its upper surface was above the elements for forming the CNT channels, which were each 1 mm in height. As a result, PDMS could be poured into the mold and form the channels without overflowing. We also rounded some sharp corners in the design with a 1 mm fillet to allow for easier removal of the PDMS substrate. Lastly, the serpentine structures for the CNT channels were moved closer together to create a more compact sensor. Shown below in Figure 2 is the second iteration of our mold showcasing the above changes.

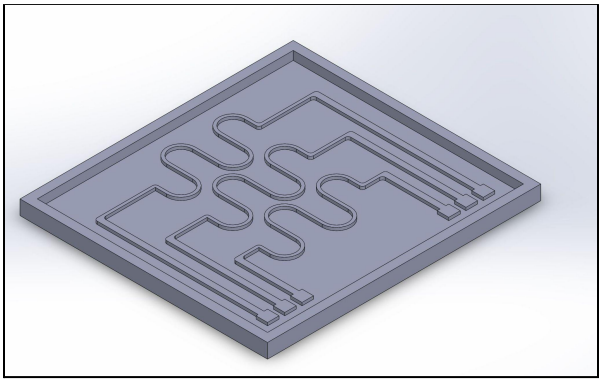

Figure 2. Second SolidWorks model of the mold, including a higher lip and additional fillets.

This second iteration worked relatively well, but minor changes were made to enhance the design even further. These minor changes included adding the reference channel at the bottom of the sensor, shown below in Figure 3, to provide a baseline value for the experimental results. Other minor changes include decreasing the cross-sectional dimensions of the CNT channels to 0.5 mm x 0.5 mm and decreasing the depth of the sensor and channels to 1 mm.

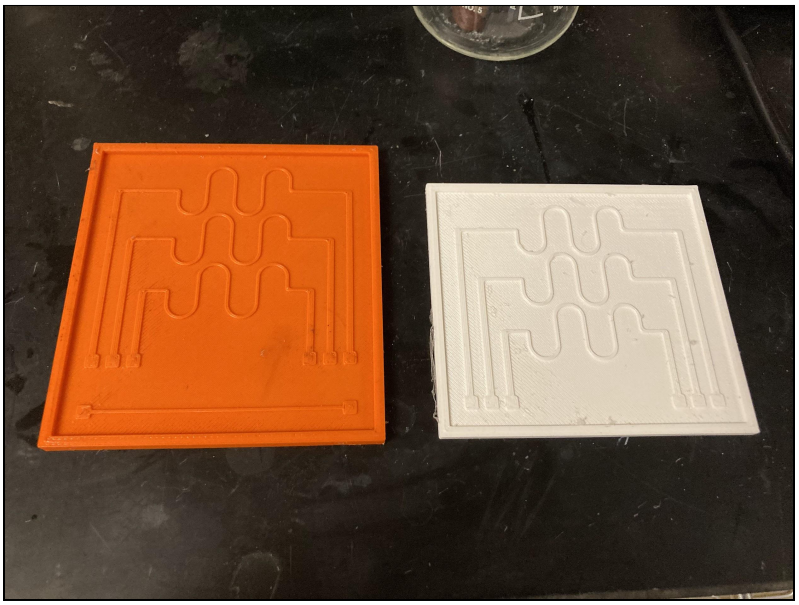

Figure 3. Two sensor molds, including the last iteration with a reference channel on the left.

Fabrication Steps-

When using the 3D molds, the fabrication of the sensor followed a sequential process. This process began with the pouring of the PDMS substrate. Several steps had to be taken to cast the substrate for the sensor. First, raw PDMS had to be mixed with a hardening agent. The ductility of the substrate was inversely proportional to the amount of hardening agent mixed into the PDMS, but the ratio by weight of PDMS to hardening agent had to be between 5:1 and 50:1. A mixture with a lower ratio than 5:1 would be too brittle for practical use, and a mixture with a

higher ratio than 50:1 would not set. A mixture with an intermediate ratio of 10:1 was used almost exclusively.

Once our ratio was determined, the raw PDMS and the hardening agent were measured and poured into a test tube after which they were mixed vigorously for approximately one minute to ensure a homogeneous mixture. Because of this mixing, a significant number of air bubbles were suspended in the liquid, which would have reduced the quality of the final substrate if they were not removed. To remove the air bubbles, the test tube was placed into a vacuum chamber. With the chamber evacuated, the bubbles rose to the top of the PDMS mixture; they were then popped by breaking the seal on the chamber, allowing air to rush into it and break the bubbles. This process had to be repeated several times in order to pop most of the bubbles, and the last of the bubbles were popped by removing the tube from the chamber and tapping the tube aggressively.

Before pouring the mixture, a lubricating spray was applied to the mold to ensure the easy removal of the substrate when it cured. The initial layer of the sensor was poured onto the mold, which itself was held in a petri dish. To ensure that no additional bubbles were captured in the mixture while pouring, it was poured slowly and from a low height. While the mixture remained in the liquid state, it flowed throughout the mold, but it was quite viscous, and to cover the mold, the mold had to be turned and rotated to ensure an even distribution of PDMS. Afterwards, the petri dish was covered to ensure that no dust or other foreign objects fell onto the substrate, and the PDMS was left to cure for multiple days; alternatively, it could have been placed in a hot oven to cure in a much shorter time. After curing, the PDMS substrate was removed from the mold.

Conversely, a similar substrate could be fabricated by using a laser cutter. For this process, rather than pouring the PDMS mixture into a 3D printed mold, the mixture had to be poured into a petri dish to form a PDMS layer for the sensor's substrate. To ensure the proper thickness was achieved, the volume of the PDMS poured into the dish and the diameter of the dish were measured. The volume of PDMS was calculated assuming a density of 1 g/cm^3, and with the volume of PDMS and diameter of the dish, the thickness was calculated. After the PDMS was poured, the mixture was degassed and fully cured before the channels were cut with the laser cutter. The original 3D mold design was converted from an .svg file to K40 whisperer, the compatible software for the laser cutter. Then, the laser cutter could be used to cut channels in the PDMS layer following the pattern from the mold design, thereby producing a sensor comparable to that produced from the mold. Before the channels could be cut, multiple trials were necessary to determine the ideal power and speed settings for the laser cutter. After these were determined, the channels were cut and cleaned.

Once the substrates were cured, they were fashioned into complete sensors in identical ways. In each substrate, the channels had to be filled with CNTs to form the conducting elements of the sensor. To fill the channels, a paste was made with CNTs mixed in PDMS. The mixing was accomplished by placing a test tube containing the mixture in a sonicator until a uniform mixture was achieved. Then, a curing agent was added to the paste and hand mixed, and the complete mixture was placed in the vacuum chamber to remove any air bubbles suspended in it. After this, a miniature spatula was used to transfer the CNT paste into the channels in the substrate. Once they were filled, the entire substrate was again placed into the vacuum chamber to remove air bubbles that were captured during the filling process. Once the substrate was removed from the chamber, the CNT paste was left to cure. This process was repeated as necessary until enough

CNTs were placed into the channels so that their resistance after curing was as low as possible, generally around 20kΩ. A completed sensor is shown below in Figure 3.

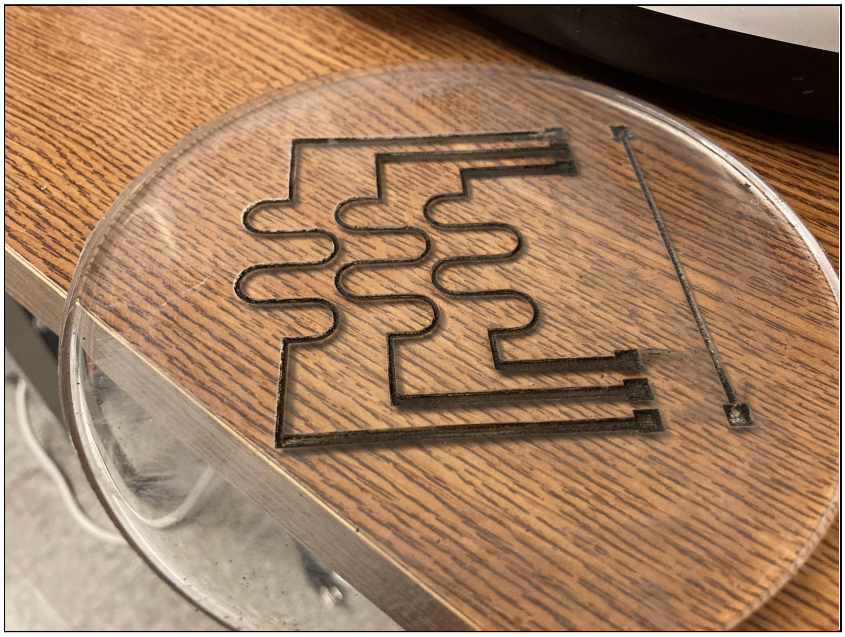

Figure 4. A laser cut sensor filled with CNT mixture, including a reference bar shown on the right.

Results

Following the fabrication of the sensors, several techniques were used to help to evaluate their effectiveness. First, Scanning Electron Microscope (SEM) images were taken of select CNT channels to evaluate how the CNTs were oriented in the channels after they were filled. Figure 4 below shows two 10,000x SEM images of the same channel using a Secondary Electron Scanning (SE) mode. This mode was chosen to take the images because it enables better topographical resolution, rendering the CNTs at the surface of the channel observable. In considering these images, it should be noted that charging played a large role in reducing the resolution of the SEM images because of the conductive nature of the channels. Additionally, the uneven surface of the channels further degraded the resolution and introduced edge effects. In the

future, methods such as sputter coating the surface of the CNT channel before imaging could be employed to help improve the resolution and gain even more insight into the CNTs' orientation.

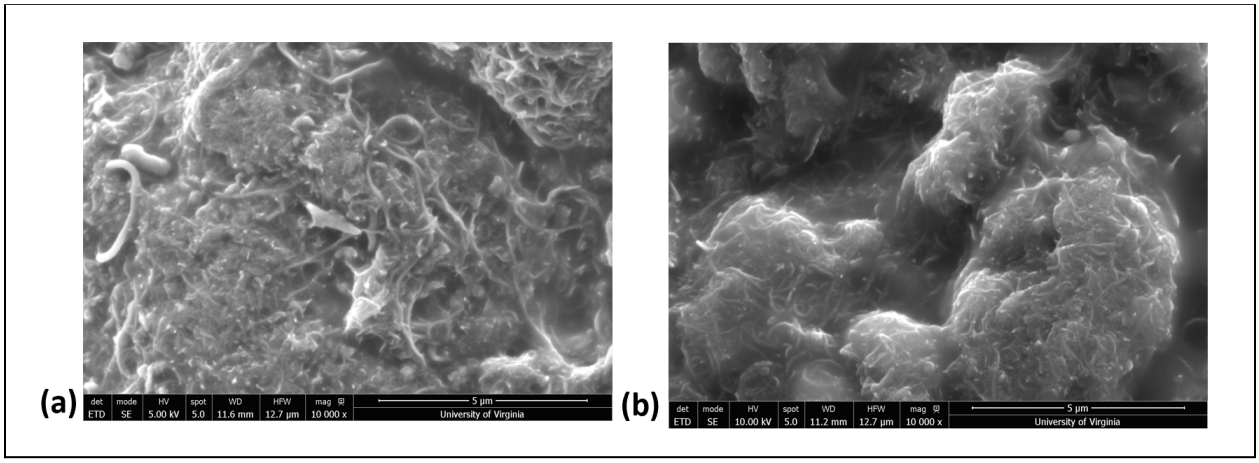

Figure 5. SEM images of a filled CNT channel.

Despite these drawbacks, the CNTs can clearly be observed in Figure 4. They are the bright, wire-like features visible in both images. Additionally, it should be noted that these nanotubes are randomly oriented and cross link at several points. The cross linking of the nanotubes is an excellent indication that the channel will be able to conduct current. This helped to confirm that suspending nanotubes in a mixture of PDMS and transferring that mixture to prefabricated channels in a sensor's substrate is an effective way to create a flexible conducting element.

With this visual confirmation that the channels were conductive, the change in the resistances of the sensors were measured as a function of temperature. For each sensor, its temperature was varied from room temperature, 25 °C, to 50 °C using a hot plate. The resistance of its reference channel was then measured at increments of 5 °C. The reference channel was chosen for this measurement because it exhibited the least resistance of all the channels and was least likely to be negatively impacted by gaps in the CNT channels. For each sensor, the percent

change in resistance divided by the initial resistance at 25 °C was plotted versus temperature, as shown in Figure 6.

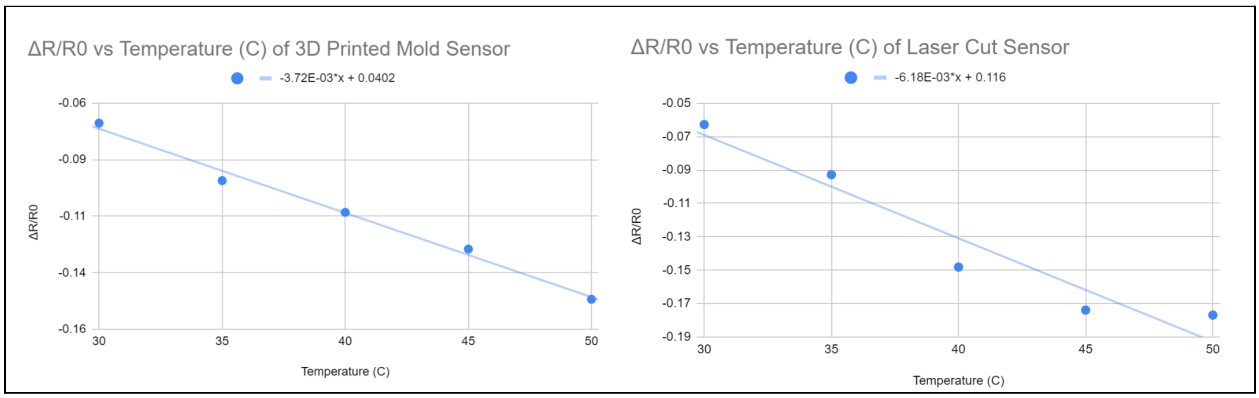

Figure 6. Plots of change in resistance divided by initial resistance versus temperature for two sensors.

As seen above, both sensors displayed a negative relationship between the percent change in resistance and temperature. For the 3D printed sensor, α was -0.00372, and for the laser cut sensor, α was -0.00618. The difference in α can likely be explained by the subjective way in which the channels were filled with CNTs. Both sensors were filled in by hand which is not a consistent filling method. Regardless, both values indicate that the overall resistance of the sensor decreases as temperature increases. Thus, if the sensor was attached to a voltage supply, it would draw increasing amounts of current as its temperature increased.

While both fabrication methods produced a sensor exhibiting this general trend, the data seems to suggest characteristic differences between the sensors. According to the graphs above, the laser cut sensor exhibited a much sharper downward trend as the temperature increased. For most of the temperatures tested, the percent change in the resistance for the laser cut specimen was greater than the corresponding percent change in the 3D printed specimen. Although this may seem odd, there are several potential explanations for this discrepancy. One explanation is the manner in which the resistances were measured. For each sensor, the resistance was

measured by hand, so deviations in the placement of the resistance meter could have resulted in different measurements. Additionally, the heat of the specimens was manipulated by a hot plate in a fume hood, where the convection of the circulating air could have affected the sensors differently. Despite the observable differences in the behavior of the sensors, the downward trend in the data for each indicates that they can be employed as temperature sensors. For such use, each sensor would need to be calibrated and connected to a voltage supply and a resistance sensor, but these additions were beyond the scope of our research.

An additional finding was the relative resistances of the two sensors. In general, the resistance of the sensor made with the 3D printed mold was lower than that of the laser cut sensor. The initial resistance at room temperature for the 3D printed sensor was 16.65 kΩ, whereas it was 28.08 kΩ for the laser cut sensor. One explanation for this deviation in the initial resistance of the sensors is the difference in the channel depths. The 3D printed sensor had a consistent channel depth of 0.5mm, while the laser cut channel was less deep. Because of that decrease in depth, less CNTs could be placed into the laser cut sensor, meaning that there were less opportunities for contact between the nanotubes. This decrease in contact between the CNTs restricted current flow, thereby causing an increase in the overall resistance of the sensor and a decreased sensitivity to temperature change. This explains the greater deviation of the laser cut sensor measurements from the line of best fit; the 3D printed sensor produced more precise results due to its heightened sensitivity.

Conclusion

This research culminated in two primary results. First, it was demonstrated that skin-like temperature sensors can be designed with PDMS substrates housing CNT conducting elements.

Additionally, it was demonstrated that both 3D printed molds and laser cutting processes can be used to fabricate the PDMS substrates for such sensors, though differences in the resulting sensors may be present due to the different manufacturing methods. Combined, these results provide valuable information for other researchers as they seek to develop skin-like sensors further.

Several steps could be taken to build upon the results of this work. First, more sensors could be developed with these methods to investigate whether sensors such as these are able to provide consistent results. For our design specifically, additional work would be necessary to fine-tune the laser cutter to provide the optimal channel depth in the substrate. Secondly, future work is necessary to measure the effects of pouring a layer of PDMS on top of the sensor upon the changes in resistance as a function of temperature. The addition of such a layer would likely be necessary to protect the sensing elements during actual operation. Lastly, the sensor should also be tested for its viability as a temperature sensor. Typically, resistance also varies with geometrical changes, so this design may be able to serve that purpose as well.

Acknowledgements

Special thanks to our advisor, Professor Baoxing Xu, for his instruction, advice, and assistance over the course of this project. Additional thanks to Mengtian Yin for the selfless and extensive aid that he provided for the several months over which this project was completed.

References

Hammock, M. L., Chortos, A., Tee, B. C.-K., Tok, J. B.-H., & Bao, Z. (2013). The evolution of electronic skin (e-skin): A brief history, design considerations, and recent progress. Advanced Materials, 25(42), 5997–6037. https://doi.org/10.1002/adma.201302240

Ray, T. R., Choi, J., Bandodkar, A. J., Krishnan, S., Gutruf, P., Tian, L., Ghaffari, R., & Rogers, J. A. (2019). Bio-integrated wearable systems: A comprehensive review. Chemical Reviews, 119(8), 5461–5533. https://doi.org/10.1021/acs.chemrev.8b00573

Xu, Baoxing (2021). Lecture 1: Design and Manufacturing of Wearable Devices. https://collab.its.virginia.edu/access/content/group/4f2ad8a8-f9fa-4f06-b247-eb3f368e0901/Lecture%201.pdf